Available online at www.sciencedirect.com
SCIENCE DIRECT®
Developmental Biology 280 (2005) 162–176
DEVELOPMENTAL BIOLOGY
www.elsevier.com/locate/ydbio

Genetic screens for genes controlling motor nerve–muscle development and interactions

Joanne Birely, Valerie A. Schneider, Evelyn Santana, Roland Dosch[1], Daniel S. Wagner[2], Mary C. Mullins, Michael Granato*

Department of Cell and Developmental Biology, University of Pennsylvania School of Medicine, Philadelphia, PA 19104-6058, USA

Received for publication 7 December 2004, revised 10 January 2005, accepted 12 January 2005

Abstract

Motor growth cones navigate long and complex trajectories to connect with their muscle targets. Experimental studies have shown that this guidance process critically depends on extrinsic cues. In the zebrafish embryo, a subset of mesodermal cells, the adaxial cells, delineates the prospective path of pioneering motor growth cones. Genetic ablation of adaxial cells causes profound pathfinding defects, suggesting the existence of adaxial cell derived guidance factors. Intriguingly, adaxial cells are themselves migratory, and as growth cones approach they migrate away from the prospective axonal path to the lateral surface of the myotome, where they develop into slow-twitching muscle fibers. Genetic screens in embryos stained with an antibody cocktail identified mutants with specific defects in differentiation and migration of adaxial cells/slow muscle fibers, as well as mutants with specific defects in axonal pathfinding, including exit from the spinal cord and pathway selection. Together, the genes underlying these mutant phenotypes define pathways essential for nerve and muscle development and interactions between these two cell types.

Keywords: Zebrafish; Mutagenesis; Genetic screen; Motor neuron; Adaxial cells; Slow-twitch muscle fibers; Axonal pathfinding; Axonal guidance; Motoneurons

Introduction

Genetic screens to uncover genes critical for cell migration and axonal guidance have been extremely successful in flies and worms. There, antibody-based or reporter-based screens have identified key genes for axonal guidance towards and across the midline (Seeger et al., 1993; Zallen et al., 1999), guidance along the anterior–posterior axis (Wightman et al., 1997), motor axon guidance (Kraut et al., 2001; Van Vactor et al., 1993) and guidance of specialized cell types, including canal associated neurons (Forrester and Garriga, 1997) or pharyngeal axons (Morck et al., 2003). In vertebrates, comparable genetic screens using antibodies or reporter lines to identify essential genes are limited by the greater complexity of the vertebrate nervous system and the logistic requirements to perform such screens. Gene trapping strategies in mice and genetic screens in zebrafish have been successfully used to identify genes with critical roles in cell migration and axonal guidance (Beattie et al., 1999; Granato et al., 1996; Karlstrom et al., 1996; Leighton et al., 2001). However, of these screens, only two were designed to identify genes critical for motor axonal guidance. In the first, Beattie et al. performed a small scale antibody-based parthenogenetic screen using diploid embryos (Beattie et al., 1999), while in the second, large-scale screen, pre-selected mutants with defects in locomotion were re-screened using antibodies (Granato et al., 1996). Together, these screens identified only five genes essential for motor axon guidance (reviewed in: Beattie, 2000).

* Corresponding author. Fax: +1 215 898 9871.
E-mail address: granatom@mail.med.upenn.edu (M. Granato).
[1] Current address: Universite de Geneve, Switzerland.
[2] Current address: Department of Biochemistry and Cell Biology, Rice University.

0012-1606/$ - see front matter © 2005 Elsevier Inc. All rights reserved.
doi:10.1016/j.ydbio.2005.01.012

Recently, a large-scale insertional mutagenesis screen in the zebrafish has identified 315 embryonic essential genes (Amsterdam et al., 2004). Surprisingly, mutations in well-studied axonal guidance genes such as Robos, Slits and Semaphorins are absent from this collection. Moreover, mutations in the zebrafish *astray* (*robo2*) and *robo3* genes, previously identified in the Tuebingen large-scale screen, result in partially viable animals (M. G. unpublished results and Fricke et al., 2001). These results, combined with the low number of motor axon genes recovered in the previous locomotion screen, suggest that mutations in genes critical for motor axonal guidance may not result in embryonic lethality or easily detectable locomotion defects. Consistent with this notion, we find that null mutant embryos for the *unplugged* gene, which is essential for motor axonal pathway selection, initially display a locomotion defect, but recover from this within 1 day and develop into viable adults (Zhang et al., 2001). Similarly, *stumpy* and *topped* mutants, in which motor axon guidance is severely compromised, display no other discernible phenotype, and mutant alleles for each of these genes are homozygous viable (Beattie et al., 2000; Rodino-Klapac and Beattie, 2004).

To identify additional genes essential for motor axon guidance, we performed an antibody-based screen using diploid embryos. We focused on the primary spinal motoneurons, because there are only three per hemisegment, and because they are the first to pioneer into the periphery (reviewed in: Beattie, 2000). Growth cones of the three primary motoneurons initially share a path into the periphery along the medial surface of the somites (Bernhardt et al., 1998; Eisen et al., 1986). At the distal end of this shared or common path, all pioneering growth cones contact a group of specialized cells called the muscle pioneers (Felsenfeld et al., 1991; Melançon et al., 1997). After reaching this choice point, they pause before selecting cell-type specific paths to ventral, dorsal and medial myotomal regions (Eisen et al., 1986; Myers et al., 1986; Westerfield et al., 1986). We have previously shown that growth cone migration along the common path, as well as pathway selection at the choice point, critically depends on signals provided by dorsal adaxial cells (Zeller and Granato, 1999; Zeller et al., 2002; Zhang and Granato, 2000). Adaxial cells form in response to Hedgehog (Hh) signals and represent a small population of myotomal cells that develop into slow-twitching muscle fibers (Currie and Ingham, 1996; Devoto et al., 1996). Intriguingly, dorsal adaxial cell delineate the prospective common path on the medial somite surface and migrate to the lateral somite surface as the first motor growth cones enter the common path (Devoto et al., 1996; Zeller and Granato, 1999). While there is clear genetic evidence that adaxial cells play a critical role in providing guidance signals to motor growth cones, little is known about the differentiation and migration of these cells, or the nature of guidance signals they provide. Thus, we used antibodies to visualize motor axonal trajectories and adaxial cells/slow muscle fibers in a genetic pilot screen to identify genes that govern the development of motor axons and adaxial cells/slow muscle fibers, as well as for genes critical for interactions between these cell types.

Here, we report on the isolation of 15 mutants which cover a broad spectrum of phenotypes but can be divided into three categories. Through phenotypic analyses, chimera analyses and molecular cloning of some of these mutants, we conclude that (1) adaxial cells play a pivotal role in motor axonal guidance; (2) antibody-based screens can identify mutations in presumptive guidance genes, without associated defects in morphology or locomotion; (3) some of the mutants provide key entry points into biological processes not well understood, such as differentiation of muscle cell types towards their unique fiber type profile or axonal guidance towards and through segmental central nervous system exit points.

Materials and methods

Mutagenesis, fish maintenance and breeding

Zebrafish were raised and maintained as previously described by Mullins et al. (1994). Embryos were staged as reported in Kimmel et al. (1995). ENU mutagenesis was performed as described in Mullins et al. (1994) and in Dosch et al. (2004).

Screening procedure

26–28 hpf (hours post fertilization) F3 embryos were anesthetized (0.01% Tricaine), fixed overnight in 4% PFA in 0.1 M phosphate buffer, pH 7.4 (81 mM Na_2HPO_4, 19 mM NaH_2PO_4, pH 7.4) plus 1% DMSO, and then washed several times in 0.1 M phosphate buffer pH 7.4. Fixed embryos were dehydrated through a MeOH series and stored in 100% MeOH at −20°C. Stored embryos were then transferred into prechilled 100% acetone and incubated for 30 min at −20°C, and then washed several times with incubation buffer (0.2% BSA, 0.5% triton-X in 0.1 M phosphate buffer, pH 7.4). All subsequent antibody stainings with primary and secondary antibodies were performed in 24 well plates. Stained embryos were transferred into Vectashield mounting medium (Vector Laboratories). From each clutch, 12 embryos were screened for defects using a Leica MZFLIII stereomicroscope equipped with epifluorescence.

Antibody stainings and α-bungarotoxin labeling

Antibody stainings and cross sections were performed as previously described in Zeller et al. (2002). The following primary antibodies were used: znp-1; (1:200, Antibody Facility, University of Oregon, Trevarrow et al., 1990); F59 (1:10, kindly provided by F. Stockdale, Crow and

Stockdale, 1986; Devoto et al., 1996); F310 (1:200, generously provided by Dr. N. Rubinstein, Crow and Stockdale, 1986); prox-1 (Glasgow and Tomarev, 1998); 4D9 (1:200; Hatta et al., 1991). Stainings were detected using AlexaFluor 488 or AlexaFluor 594 conjugated anti-mouse secondary antibodies diluted in incubation buffer (1:500; Molecular Probes, Eugene, OR). To avoid cross reactivity in the F310/F59 double labeling, we directly labeled F310 using the Zenon One Kit (Molecular Probes) according to the manufacturer's instructions. Clustered AChRs were visualized using AlexaFluor 594 conjugated α-bungarotoxin (10 μg/mL, Molecular Probes). Embryos were imaged using a LSM510 confocal microscope (Zeiss). Images were processed using Adobe Photoshop and Adobe Illustrator.

Chimeric embryos

Chimeric embryos were generated and analyzed as previously reported in Zeller and Granato (1999).

Molecular biology

To clone *unplugged* cDNAs from *p31cd* mutant embryos and N-cadherin cDNAs from *p79emcf* mutants, RNA was extracted from 28 hpf wild-type and mutant embryos and used for RT-PCR. The AccessQuick RT-PCR system (Promega) was used with gene specific primers to reverse transcribe and amplify corresponding cDNAs in fragments. The amplification products were cloned into the pCR2.1 vector (Invitrogen), sequenced and analyzed using MacVector 7.1.

Results and discussion

We performed a standard three-generation screen to identify zygotic genes essential for adaxial cell/slow muscle fiber and motor axon development. At 26 hpf, motor axons have migrated into the periphery and selected their cell-type specific path, while adaxial cells have migrated from the medial to the lateral surface of the myotome, forming a single layer of slow-twitching muscle fibers. Embryos were double stained to visualize motor axons (znp1) and adaxial cell/slow muscle fibers (F59) and were then scored for defects in axonal pathfinding, adaxial cell differentiation and migration (Fig. 1). We screened embryos from a total of 1703 crosses derived from 423 families, scoring a total of 498 mutagenized genomes. This represents 12.5% and 17% of the genomes analyzed in the large-scale Tuebingen and Boston screens, respectively (Driever et al., 1996; Haffter et al., 1996). We identified 17 mutants and characterized 15 mutants with specific defects (two mutants displayed general necrosis defects and were discarded). These 15 mutants were subdivided into three phenotypic groups: mutants with defects only in adaxial cells (6), mutants with defects in adaxial cells and motor axons (6) and mutants with defects only in motor axons (3; Table 1). We performed a limited number of complementation tests between mutants with similar phenotypes, as well as with some of the mutants previously identified in the Tuebingen and Boston screens (Table 1). This revealed that we identified two new mutant alleles of *deadly seven*, one new allele of *parachute*, as well as one new allele of *unplugged*, one of a handful of previously identified genes essential for motor axonal

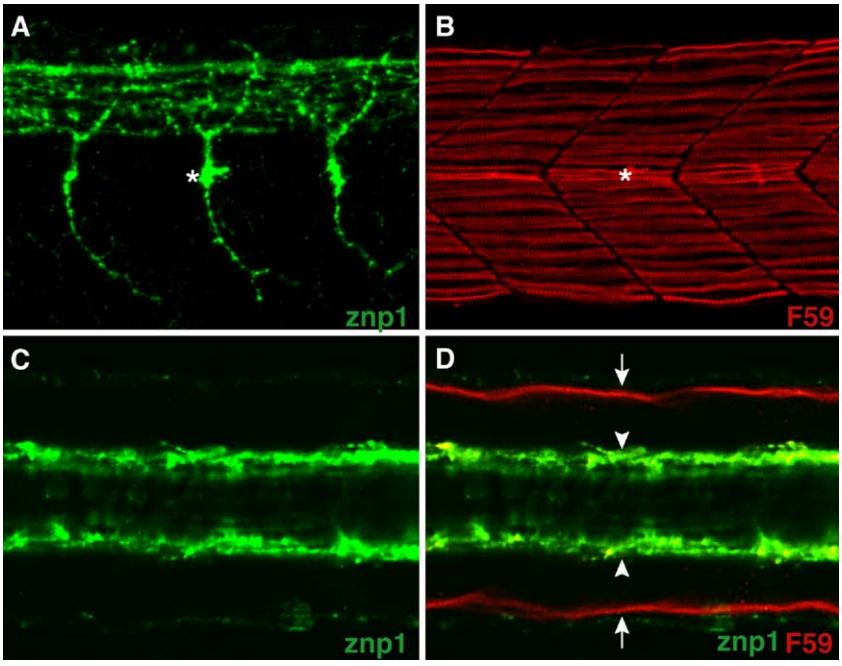

Fig. 1. Lateral (A, B) and dorsal (C, D) views used to screen embryos for defects in motor axon guidance (A), adaxial cells/slow muscle fiber development (B) or migration (C, D). Asterisks in panels A and B indicate the region of the choice point, where motor growth cones make contacts with muscle pioneers. (C, D) Adaxial cells migrate from their medial location adjacent to the spinal cord (in green, arrowheads) to the lateral surface of the myotome (red, arrows).

Table 1
Mutant phenotypes

Mutant	Phenotype	Gene	Com.[a]
Mutants with adaxial cell defects			
p20caed	F59 staining disorganized at 26 hpf; immotile from 22hpf onwards; no heartbeat at 48 hpf and reduced/no axial muscle birefringence; affects slow and fast muscle		*p32cree*, *p37caed*
p37caed	F59 staining disorganized at 26 hpf; immotile from 22hpf onwards; no heartbeat at 48 hpf and reduced/no axial muscle birefringence; affects slow and fast muscle		*p20caed*
p32cree	F59 staining disorganized. At 48 hpf reduced/no axial muscle birefringence, and embryos are immotile; affects slow and fast muscle		*p20caed*
p17cfem	F59 staining disorganized and individual muscle fibers look thinner; at 23 hpf embryos move spontaneously; at 36 hpf mutants are immotile, heart is beating but no blood flow; affects slow and fast muscle		
p1cpej	F59 positive muscle fibers are detached from vertical septa and end with knob-like structure. Specific to slow muscle fibers. No other morphological or behavioral defects	*stretched-out* (*sot*)[b]	
p37cpej	F310 positive muscle fibers are also F59 positive. All slow muscle cells are present and positive for prox-1 and 4D9, but do not express F59. From 28 hpf on, embryos can be sorted by motility	*popeye's sister* (*pop*)[b]	
Mutants with adaxial cell and motor axonal defects			
p48egcq	F59 positive fibers are often detached from vertical septa or missing, forming gaps. Motor axons are branched. Boundaries of first seven somites are reduced or absent. Allelic to p76emcf	*deadly seven* (*Notch1α*)	
p76emcf	F59 positive fibers are often detached from vertical septa or missing, forming gaps. Motor axons are branched. Boundaries of first seven somites are reduced or absent. Allelic to p48egcq.	*deadly seven* (*Notch1α*)	
p79emcf	Many F59 positive fibers fail to migrate radially. Motor axons are branched. Hindbrain defects.	*parachute* (*cdh2*)	
p32cqeg	F59 positive muscle fibers are disorganized, but muscle pioneers present. Motor axons are short and often branched. Notochord undifferentiated, disorganized hindbrain, retinotectal projections abnormal		*bashful*
p71cfem	In many hemisegments one or more F59 positive muscle fibers are missing. Motor axons are often short or missing. Somites are U-shaped	*chameleon* (*disp1*)	*you-too* (*gli2*), *sonic-you* (*shh*)
p82emcf	Motor axons are short and branched. Notochord is undulating but cells appear differentiated, somites slightly U-shaped		
Mutants with motor axonal defects			
p31cd	Motor axons stall or branch at choice point	*unplugged* (*unp*)	
p24cree	Two phenotypes: first, motor axons exit at ectopic location from the spinal cord, resulting in many somitic hemisegments innervated by two ventral roots. Second, motor axons branch at or after the choice point. Allelic to p55emcf	*sidetracked* (*set*)[b]	
p55emcf	Two phenotypes: first, motor axons exit at ectopic location from the spinal cord, resulting in many somitic hemisegments innervated by two ventral roots. Second, motor axons branch at or after the choice point. Allelic to p24cree	*sidetracked* (*set*)[b]	

[a] Complements the following mutants.
[b] These mutants were given a new gene name because no comparable phenotype had previous been reported. For all other un-named mutants, we could not exclude the possibility that mutant alleles had previously been identified in other screens.

pathfinding in the zebrafish (Granato et al., 1996; Jiang et al., 1996; van Eeden et al., 1996). However, it was not possible to perform complementation testing with the large number of mutants and somite mutants previously identified in the Tuebingen and Boston screens, so we cannot rule out that some of our mutants may be alleles of previously identified mutants. While the lack of new mutant alleles of *diwanka* or *stumpy*, two other well-characterized axonal guidance mutants, likely reflects the small scale of our screen, the identification of a new *unplugged* allele, as well as the isolation of new mutants with axonal or adaxial cell defects, validates our screening procedure.

Mutants affecting adaxial cell development

We identified 6 mutants with defects only in adaxial cell/slow muscle fiber development. Adaxial cells originate on the medial surface of the myotome in response to Hh signals and can be subdivided in later-migratory cells which develop into muscle pioneers located at the region of the horizontal

myoseptum, and in migratory adaxial cells, which migrate radially to the lateral surface of the myotome, where they form a superficial layer (reviewed in: Stickney et al., 2000). Muscle pioneers and migratory adaxial cells develop into mononucleated, slow muscle fibers, which all express a slow myosin heavy chain protein recognized by the F59 antibody. In wild-type embryos, F59 staining emphasizes the striated or sarcomeric character of skeletal muscle (Figs. 2B, G). Four mutants (*p20caed*, *p37caed*, *p32cree* and *p17cfem*) display a similar phenotype, characterized by a diffuse appearance of the F59 staining. Specifically, F59 immunoreativity appears more diffuse throughout the muscle fiber rather than restricted to contractile filaments, suggesting that sarcomere organization is disrupted (Fig. 2D and data not shown). In consequence, the nucleus is now visible as a F59 negative area surrounded by F59 immunoreactivity. At 48 hpf, all four mutants display reduced or no axial muscle birefringence, indicating that both axial muscle fiber types, fast and slow, are affected (data not shown). Consequently, all four mutants display locomotion defects, and three of them also display

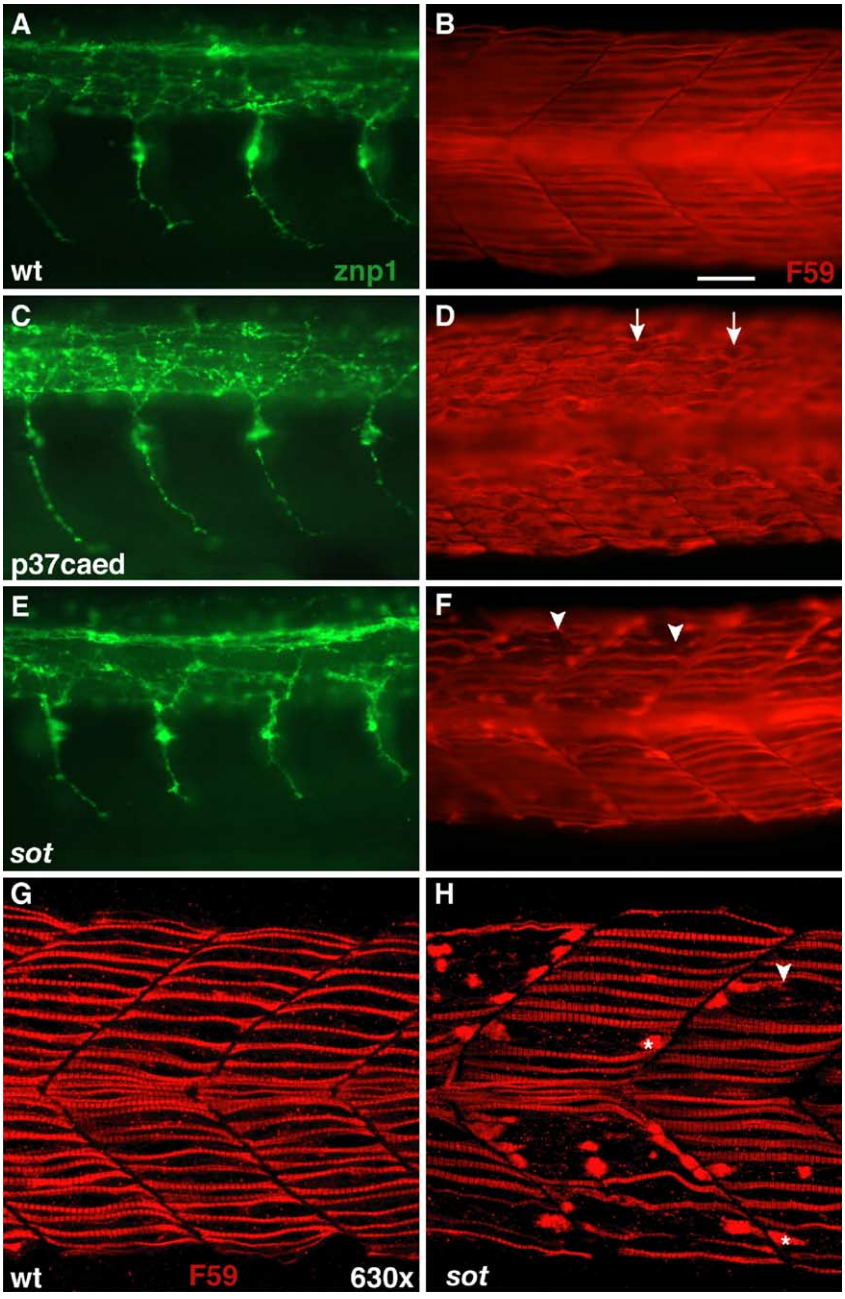

Fig. 2. Lateral views of wild-type (A, B, G) and mutant embryos (C–F, H) double stained with F59 for adaxial cells/slow muscle fibers and znp1 for motor axons. In panel D, the arrows point to nuclei of slow muscle fibers, not visible in wild type. In panels F and H, arrowheads point to broken fibers, and asterisks indicate presumptive fiber residues attached to the vertical somite boundary. (G, H) Higher magnification confocal images of wild-type and *sot* mutant embryos stained with F59.

cardiovascular defects (Table 1). In all four mutants, motor axonal trajectories are unaffected (Fig. 2C), suggesting that muscle defects are not caused by an overall developmental delay, and are not due to general, e.g. metabolic, defects. Rather, in these mutants, F59 immunoreactivity is present but disorganized, suggesting that mutant muscle fibers produce contractile elements but fail to assemble them into functional sarcomeres. The phenotype of these mutants is similar to that observed in a group of mutants previously identified in the Tuebingen screen (Granato et al., 1996). Although further characterization of these mutants is required, they are likely to serve as a valuable model in which to study the assembly of contractile elements into highly organized sub-cellular structures, the sarcomeres.

In two mutants, a different aspect of adaxial cell/slow muscle fiber development is affected. In *stretched-out* (*sot*) mutants, motor axons are unaffected, but somites contain broken or disrupted slow muscle fibers (Figs. 2F, H). In 26 hpf wild-type embryos, F59 stains approximately 10 muscle fibers in the dorsal and ventral myotome, respectively, in addition to 2–6 muscle pioneers at the horizontal myoseptum (Devoto et al., 1996; Stickney et al., 2000). These fibers span the entire length of a somitic segment and are attached at their ends to the vertical somite boundaries (Fig. 2G). In *sot* mutant embryos, 11% of slow muscle fibers are affected (segment 9–16, $n = 200$). In many cases, almost the entire fiber is missing, and only a small round blob of F59 positive material is attached to the vertical somite boundary (Fig. 2H). In fewer cases, a longer fragment of the broken fiber is still attached to the segmental boundary (Fig. 2H). We did not observe broken fibers in the fast muscle population when assayed with a fiber type specific antibody, and we did not observe any other morphological or behavioral phenotypes (data not shown). The broken appearance of mutant muscle fibers is somewhat reminiscent of the phenotype of heterozygous *twister* mutants (Lefebvre et al., 2004). These mutants carry a hyperactive copy of the muscle specific acetylcholine receptor, which leads to prolonged postsynaptic activity and to muscular degeneration and cell death (Lefebvre et al., 2004). In contrast, 26 hpf *sot* embryos do not exhibit increased apoptosis (data not shown). Moreover, analyses of embryos derived from two heterozygous parents did not reveal any defects in F59 positive muscle fibers at 32 or 48 hpf, suggesting that mutants recovered (data not shown). One possible interpretation is that defective fibers are replaced by newly formed slow muscle fibers. This is consistent with findings that slow muscle fibers are added to the distal end of the myotome in a second, Hh independent wave between 24 and 96 hpf (Barresi et al., 2001). Thus, *sot* mutants exhibit an intriguing but subtle phenotype. Such a phenotype would certainly have gone undetected in the previous morphological screens. Moreover, the specificity and recovery of the phenotype suggest that the mutated gene plays a specific but perhaps transient role in the assembly, function or stability of slow muscle fibers.

In *popeye's sister* (*pop*) mutants, the domain of myosin heavy chain expression is altered. In lateral views, F59 positive fibers are missing at the region of the horizontal myoseptum (data not shown). To determine which fibers are affected in *pop* mutants, we stained 26 hpf wild-type and mutant embryos with the slow muscle fiber specific myosin heavy chain (sMyHC) antibody F59 and the fast muscle fiber specific myosin heavy chain (fMyHC) antibody F310. In wild-type embryos, the bulk of the myotome consists of F310 positive fast muscle fibers, while F59 positive slow muscle fibers form a single layer on the lateral surface (Fig. 3A). Confocal sections of cross-sectioned *pop* mutants revealed that individual presumptive fast muscle fibers express fast and slow myosin (F310 and F59 positive; Fig. 3B). In contrast, presumptive slow muscle fibers at the lateral surface of the myotome appeared devoid of F59 immunoreactivity (Fig. 3B). We thus asked whether the lateral population of slow muscle fibers was absent or if it failed to express slow MyHC. For this, we used two well characterized markers: the muscle specific transcription factor *prox-1*, which is expressed exclusively in slow muscle fibers (Figs. 3C, E), and the *engrailed* (*eng*) gene, which is expressed at high levels in a subpopulation of slow muscle fibers, the muscle pioneers located at the region of the horizontal myoseptum (Fig. 3G). Double antibody labelings with F59 and α-Prox-1 or F59 and 4D9 (which recognizes *Eng* protein) revealed that, in *pop* mutants, the correct numbers of mononucleated slow muscle cells are specified and that these cells properly localize to the lateral surface of the myotome (Figs. 3D, F, H). However, in *pop* mutant embryos, prox-1 and 4D9 positive slow muscle cells fail to express slow MyHC protein (Figs. 3D, F, H). Thus, *pop* does not control adaxial cell/slow muscle fiber specification, but its subsequent differentiation.

We next asked if the *pop* gene acts cell autonomously in slow muscle fibers. We generated chimeric embryos in which wild-type derived slow muscle cells reside in otherwise *pop* mutant embryos and assayed whether these slow muscle cells would express slow MyHC. Analysis of 55 clones in 7 chimeric embryos revealed that all wild-type derived slow muscle cells now express slow MyHC, consistent with a cell autonomous role of *pop* (Figs. 3I, J). We did not determine if *pop* also acts cell autonomously in fast muscle fibers.

The *pop* phenotype is distinct from phenotypes observed in mutants in which Hh signaling or downstream targets are compromised (Barresi et al., 2000; Baxendale et al., 2004; Wolff et al., 2003). Unlike in *pop* mutants where slow muscle cells are correctly specified, in the absence of Hh signaling, slow muscle fibers are not specified. Furthermore, absence of Hh signaling does not result in ectopic expression of slow MyHC in fast muscle fibers, as observed in *pop* embryos. Finally, *pop* mutants do not exhibit any other phenotypes associated with Hh signaling, such as blood circulation or motor axonal defects (van Eeden et al., 1996). Thus, the *pop* gene is unlikely to play a critical role in fiber-type induction or specification but likely functions in muscle fiber differentiation. Intriguingly, *pop* plays a

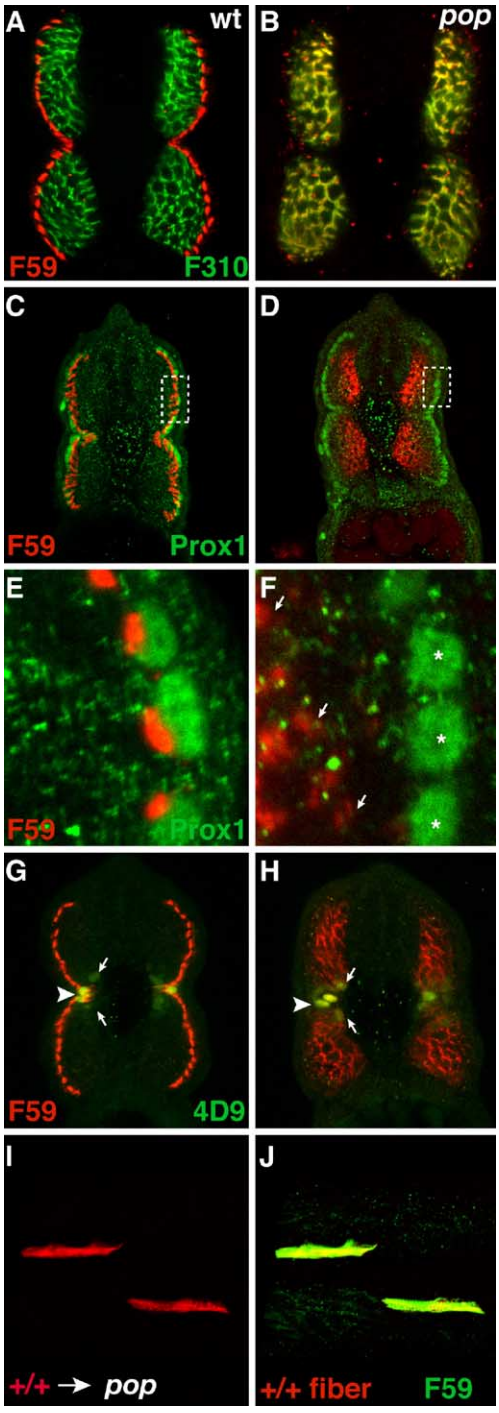

Fig. 3. Confocal cross sections of 28 hpf wild-type (A, C, E, G) and *pop* mutants (B, D, F, H) stained for fast and slow muscle fiber myosin (A, B), for Prox-1 and slow muscle fiber myosin (C–F; E, F high magnifications of areas boxed in panels C and D) and for 4D9 and slow muscle fiber myosin (G, H). In panel F, asterisks indicated Prox-1 positive slow muscle fibers, note that they do not express slow muscle myosin, which is expressed by the more medial fast muscle fibers (arrows). In panels G and H, arrowheads point to muscle pioneers and arrows to medial fast fibers (Barresi et al., 2000; Baxendale et al., 2004; Wolff et al., 2003). (I, J) A wild-type derived slow muscle fiber (red) in an otherwise *pop* mutant embryo expresses slow muscle myosin.

critical role in the slow and fast muscle lineages. In *pop* mutants, fast muscle cells incorrectly express slow MyHC, while slow muscle cells fail to express any slow MyHC. Thus, one possible role for the *pop* gene is that it functions as an activator and repressor of myogenic protein expression in both muscle fiber lineages. In slow muscle fibers, *pop* activation function would promote expression of slow MyHC, while it would function as a repressor of slow MyHC expression in fast muscle fibers. Recent studies have identified the murine transcriptional coactivator PGC-1α as a key mediator of adult muscle fiber plasticity (Lin et al., 2002). Ectopic PGC-1α expression in fast-twitch type II fibers leads to changes in mitochondrial metabolism, physiological properties and protein expression characteristic of slow-twitch type I fibers during postembryonic development. In the embryo, the *u-boot* (*blimp-1*) gene is critical for specification of slow muscle fibers in response to Hh signals (Baxendale et al., 2004). The subsequent steps of muscle fiber differentiation, including the selective expression of myosin subtypes, however, are largely obscure. Future analysis of the *pop* gene should provide molecular insights into the mechanisms by which individual muscle lineages differentiate towards their unique fiber type profile.

Mutants affecting adaxial cell and motor axonal development

We identified 6 mutants with defects in adaxial cell and motor axon development. In *p48egcq* and *p76emcf* mutants, motor axons are short and branched, while slow muscle fibers often are shorter or are completely missing, giving rise to ‘gaps’ (Figs. 4A–D). Both mutants also display irregular boundaries of the more posterior somites, a phenotype characteristic of *deadly seven* (*des*) mutants. Complementation analysis confirmed that both mutants are allelic to each other and to *des*, which encodes Notch1α (Holley et al., 2002). Mutants in *des* have previously been identified based on irregular somite boundaries (van Eeden et al., 1996) and based on motor axon defects (Beattie et al., 1999; Gray et al., 2001). The presence of multiple, independent *des* (*notch1α*) alleles in our screen (2/498 genomes) is consistent with the large number of *des* alleles identified in the Tuebingen screen (10/3857) and suggest that the *des* (*notch1α*) locus or protein is highly mutagenizable.

In mutants of *p71cfem*, a significant proportion of somitic hemisegments have shorter motor nerves or lack them completely (Figs. 4E, F). In these mutants, individual somitic segments lack one or more migratory slow muscle fibers, and all segments lack muscle pioneers (Figs. 4J–L). As a consequence, somite boundaries are U-shaped, when compared to wild-type siblings. The U-shaped somite boundary phenotype is characteristic for six previously identified *you*-type mutants, of which three, *you-too* (*gli2*), *sonic-you* (*shh*) and *chameleon* (*disp1*) also display motor axonal defects (Karlstrom et al., 1999; Nakano et al., 2004; Schauerte et al., 1998; van Eeden et al., 1996). Genetic

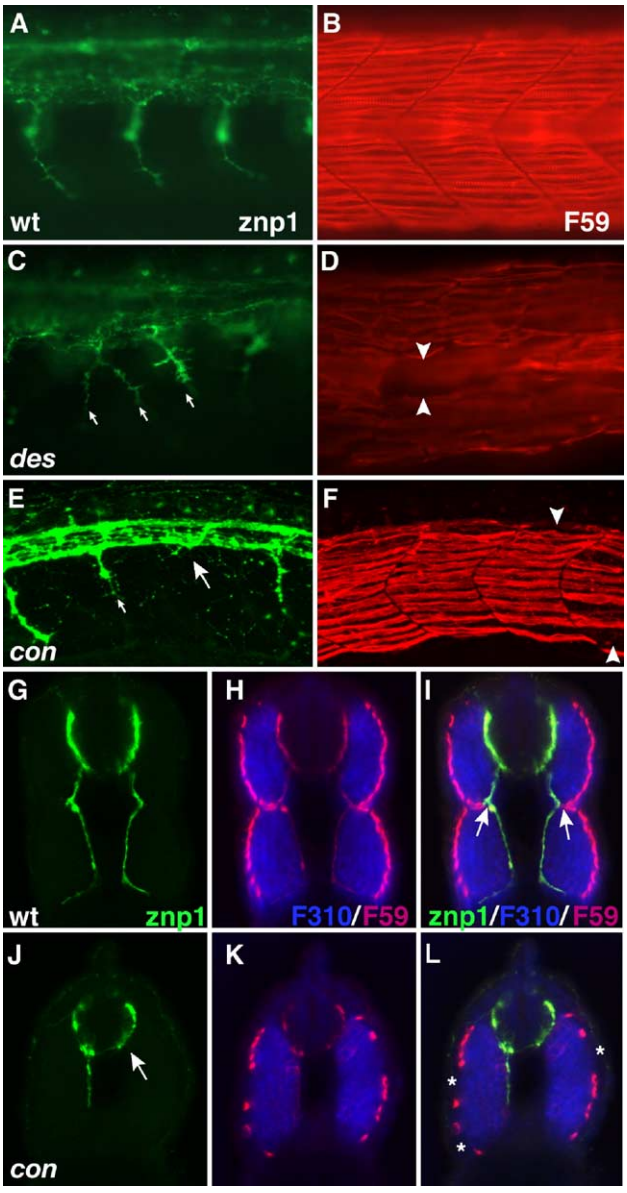

Fig. 4. Lateral views of wild-type (A, B) and mutant embryos (C–F) double stained with F59 for adaxial cells/slow muscle fibers and znp1 for motor axons. In panels C and E, arrows point to missing, short or branched axons. In panels D and F, arrowheads point to broken or missing muscle fibers. (G–L) Confocal cross sections of wild-type (G–I) and mutant embryos (J–L) triple stained with F59 for adaxial cells/slow muscle fibers, F310 for fast muscle fibers and znp1 for motor axons. In panel I, arrows point to the choice point, where motor axons contact muscle pioneers. In panel J, arrow points to missing motor axon, and in panel L, asterisks indicate missing slow muscle fibers.

crosses between *p71cfem* mutants and two *you*-type mutants revealed that *p71cfem* complements *you-too* (*gli2*) and *sonic-you* (*shh*). This made *chameleon* (*disp1*) a possible candidate for *p71cfem*. Complementation testing confirmed that *p71cfem* is indeed a new *chameleon* (*disp1*) allele.

Similar to other mutants in this class, *p79emcf* mutants display defects in adaxial cells and motor axons. Motor axons often appeared branched, and occasionally motor nerves formed a second, ectopic root through which they entered the somite (Figs. 5A, C). In many hemisegments, slow muscle fibers appeared disorganized (see below; Figs. 5B, D). In addition, *p79emcf* mutants displayed a pro-

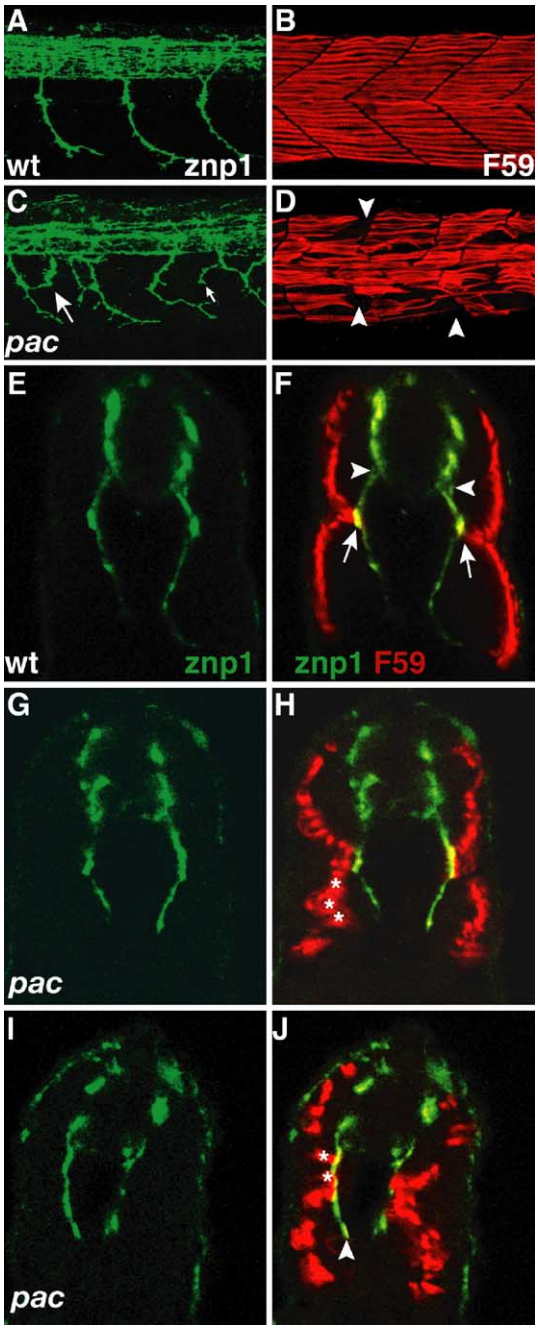

Fig. 5. Lateral confocal images of wild-type (A, B) and *pac* mutant embryos (C, D) double stained with F59 for adaxial cells/slow muscle fibers and znp1 for motor axons. In panel C, arrows point to ectopic axons (large arrow) and to axonal branches (small arrow). In panel D, arrowheads point to fibers that failed to migrate to the lateral surface. (E–J) Confocal sections of cross-sectioned wild-type (E, F) and *pac* embryos (G–J) double stained with F59 for adaxial cells/slow muscle fibers. In panel F, arrowheads point to spinal cord exit point, and arrows to the choice point. Panels G and H are an example in which ventral adaxial cells (asterisks) fail to migrate to the lateral surface. Panels I and J are an example in which dorsal adaxial cells (asterisks) fail to migrate to the lateral surface, but motor axons enter the myotome (arrowhead).

nounced defect in brain morphology, clearly visible at 24 hpf (data not shown). Specifically, the mid and hindbrain region appeared disorganized, with cell aggregates, detached from the neuroepithelium, floating in the brain ventricles. This brain phenotype is very reminiscent of the *parachute* (*pac*) mutant, which is caused by a mutation in N-cadherin (*cdh2*) (Jiang et al., 1996; Lele et al., 2002; Masai et al., 2003). Complementation analysis and subsequent sequence analysis of N-cadherin derived from *p79emcf* established that *p79emcf* is a novel allele of *pac* (*cdh2*), caused by a missense mutation (T2145G), resulting in an Isoleucine 676 to Serine (I676S) substitution in the fifth extracellular cadherin (EC5) domain. Sequencing of the mutagenized founder fish confirmed that the I676S substitution is not a polymorphism but is a mutation likely caused by the ENU treatment. The I676 residue is highly conserved among all vertebrate species examined, suggesting that it plays an important role. Previously identified N-cadherin alleles include a missense mutation in EC1 (glo^{m117}, Malicki et al., 2003), two nonsense mutations before and in EC4 (pac^{fr7}, pac^{m101B}, Lele et al., 2002) and a missense mutation in EC4 (pac^{rw95}, Masai et al., 2003). However, no mutation has previously been reported to affect the EC5 domain, and cell adhesion studies have suggested that EC5 is not essential for binding and adhesion properties of C-cadherin (Chappuis-Flament et al., 2001). We find that the $pac^{p79emcf}$ mutant phenotype equals the phenotypic strength observed in the pac^{fr7} nonsense allele, suggesting that the EC5 domain plays a critical role.

We had previously shown that adaxial cells are critical for guiding motor growth cones. For example, genetic ablation of adaxial cells prevents motor growth cones from entering into the myotome (Zeller et al., 2002). Furthermore, chimeric studies have shown that a subset of dorsal adaxial cells is responsible for enabling motor growth cones to enter the myotome (Zeller and Granato, 1999; Zhang and Granato, 2000). Intriguingly, the migration of dorsal adaxial cells is synchronized with the migration of motor axons into the somites (Zeller and Granato, 1999), raising the intriguing possibility that these two events are functionally coupled. Recently, N-cadherin has been shown to be critical for the medial to lateral migration of adaxial cells (Cortes et al., 2003). Thus, we asked if lack of dorsal adaxial cell migration in N-cad mutants correlates with axonal pathfinding defects. We first confirmed that, in $pac^{p79emcf}$ (*cdh2*) mutants, migration of adaxial cells is severely affected (Figs. 5H, J). Analysis of axonal and adaxial cell migration in $pac^{p79emcf}$ (*cdh2*) mutants revealed three phenotypic classes. Segments in which adaxial cell migration appeared indistinguishable from wild-type but motor axons were short, segments in which motor axon and adaxial cell migration was affected, and segments in which adaxial cells failed to migrate properly but motor axons extended like in wild-type embryos. We focused on this last class and examined the precise position of adaxial cells. We found several segments in which dorsal adaxial cells failed to migrate, but motor growth cones extend normally into the myotome (Fig. 5J). We conclude that N-cadherin is critical for the lateral migration of adaxial cells and for pathfinding of motor axons (Figs. 5C, D). However, these two events appear to occur independently, as motor axons enter the myotome in segments in which dorsal adaxial cells fail to migrate (Fig. 5J).

In *p32cqeg* mutants, motor axons are short and frequently branched, and in many somitic segments individual slow muscle fibers are detached from the vertical somite boundaries or missing (Figs. 6A–D). Morphologically, mutants can be identified at 26 hpf by their shortened body axis, irregular somite boundaries, local notochord degeneration and overall disorganized brain morphology, causing abnormal numbers and trajectories of reticulospinal neurons (Figs. 6E, F and not shown). These morphological defects are characteristic of a group of six genes, the 'dwarf' genes, previously identified in both large-scale screens (Odenthal et al., 1996; Stemple et al., 1996). Individual members of this group can be identified by additional phenotypes, such as the lack of muscle pioneers and defects in retinal ganglion cell (RGC) projections (Odenthal et al., 1996; Stemple et al., 1996). In *p32cqeg* mutants, muscle pioneers are present, while retinotectal projections are abnormal. In wild-type embryos, RGC axons cross the central nervous system (CNS) midline and then turn posteriorly towards the contralateral optic tectum (Fig. 6G). In *p32cqeg* mutants, RGC axons cross the midline, but rather than turning posteriorly, they project anteriorly into the forebrain (Fig. 6H). Mutants in *sleepy*, *grumpy* and *bashful* all display the same retinotectal phenotypes, but only in *bashful* mutants muscle pioneers are present (Karlstrom et al., 1996; Stemple et al., 1996). However, *p32cqeg* complements *bashful* mutants, suggesting that *p32cqeg* is a weak allele of *sleepy* or *grumpy* or represents a new mutation.

While many of the morphological defects observed in *p32cqeg* mutants have been reported for other 'dwarf' group mutants, defects in slow muscle fibers and motor axonal pathfinding have not previously been described. Defects in slow muscle fibers and motor axonal pathfinding are also a hallmark of unregulated neuromuscular activity. Specifically, in embryos expressing a mutant, hyperactive form of the muscle specific acetylcholine receptor, motor axonal pathfinding and muscle fiber development are severely impaired (Lefebvre et al., 2004). To examine if abnormal motor activity also contributes to the phenotypes observed in *p32cqeg* mutants, we used tricaine methanesulfonate (0.02%) to blocked motor activity prior to the onset of innervation (10 hpf), and at 26 hpf examined slow muscle fibers and motor axonal development in these tricaine-reared animals. In wild-type embryos, muscle fibers appeared more wavy when compared to untreated siblings, but motor activity is not required for axonal pathfinding or overall slow muscle development (Figs. 6I, J). This is consistent with previous results of tricaine treated *Xenopus* embryos (Cohen et al., 1984). Tricaine treatment of *p32cqeg* mutants did not restore brain morphology, but it did rescue motor

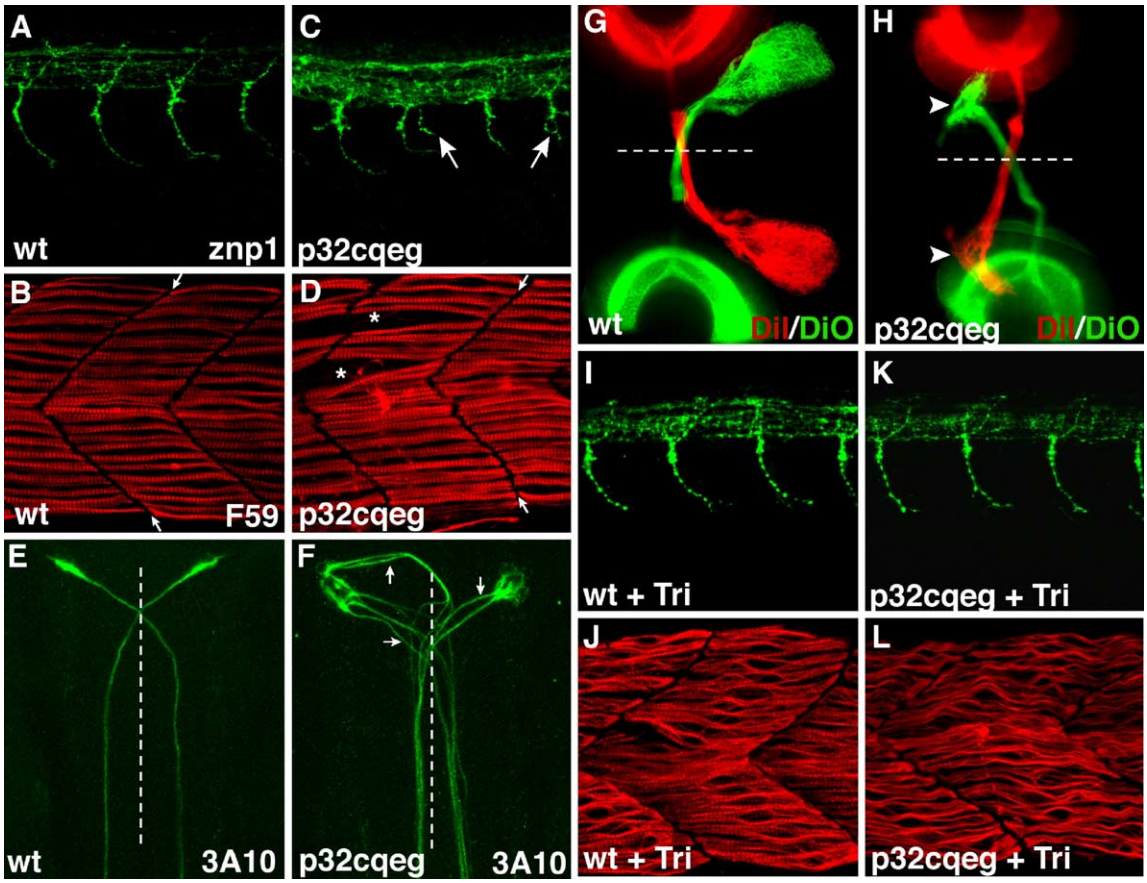

Fig. 6. Lateral confocal images of wild-type (A, B) and mutant embryos (C, D) double stained with F59 for adaxial cells/slow muscle fibers and znp1 for motor axons. In panel C, arrows point to ectopic axons and to axonal branches. In panel D, arrows point to irregular somites boundaries, and asterisks to gaps in muscle fibers. (E–F) Mutant embryos display multiple misrouted Mauthner cell axons (dashed line indicates the position of the midline, arrows point to aberrant projecting Mauthner cell axons). (G, H) Aberrant retinotectal projections in p32cqeg mutant embryos (dashed line indicates the position of the midline, and arrowheads point to aberrant optic nerve). (I–K) Blocking motor activity restores axonal and muscle defects.

axonal projections and slow muscle fibers to levels indistinguishable from tricaine-treated wild-type siblings (Figs. 6K, L). This demonstrates that the motor axonal and slow muscle fiber phenotypes observed in *p32cqeg* mutants depend on motor activity. One interpretation is that the gene mutated in *p32cqeg* plays a critical role in neuromuscular development or function. This is further supported by the notion that two of the 'dwarf' genes, *grumpy* and *sleepy*, encode laminin β1 and γ1, respectively (Parsons et al., 2002). Seven laminin genes are expressed in the mammalian neuromuscular system, where they have structural and signaling functions (Patton, 2000; Patton et al., 2001). Thus, the analysis of *p32cqeg* mutants, likely to be a member of the 'dwarf' group mutants, reveals a previously unrecognized role for 'dwarf' group genes in motor axonal pathfinding and slow muscle fiber development.

Mutants of *p82emcf* can be recognized by defects in notochord morphology. Compared to 28 hpf wild-type embryos, mutant embryos have an undulating notochord that results in a distorted body axis (Figs. 7A, B). In these mutants, adaxial cells/slow muscle fibers display only mild defects. Specifically, spacing between individual slow muscle fibers is occasionally irregular, giving raise to a gapped appearance (Figs. 7E, F). In contrast, motor axons exhibit severe pathfinding defects at the region of the choice point, either forming aberrant branches or stalling completely (Figs. 7C, D). Blocking motor activity in these mutants did not restore pathfinding, suggesting that the motor axonal defects are activity independent (data not shown). While it is unclear if the axonal defects represent a primary defect or arise as a consequence of the notochord defect, it should be noted that *no tail* mutants, which lack all differentiated notochord, establish motor axonal trajectories similar to those in wild-type animals (Fig. 5F; Halpern et al., 1993). Interestingly, the notochord defects observed in *p82emcf* mutants resemble those previously observed in *crash test dummy* (*ctd*), *zickzack* (*ziz*), *kinks* (*kik*) and *wavy tail* (*wat*), but no axonal defects have been reported in these mutants (Odenthal et al., 1996). Thus, our screen reveals motor axonal defects in a class of mutants previously noted only for defects in notochord development.

Mutants affecting only motor axonal development

We identified three mutants with specific defects in motor axon guidance. In *p31eccd* mutants, motor axons stall

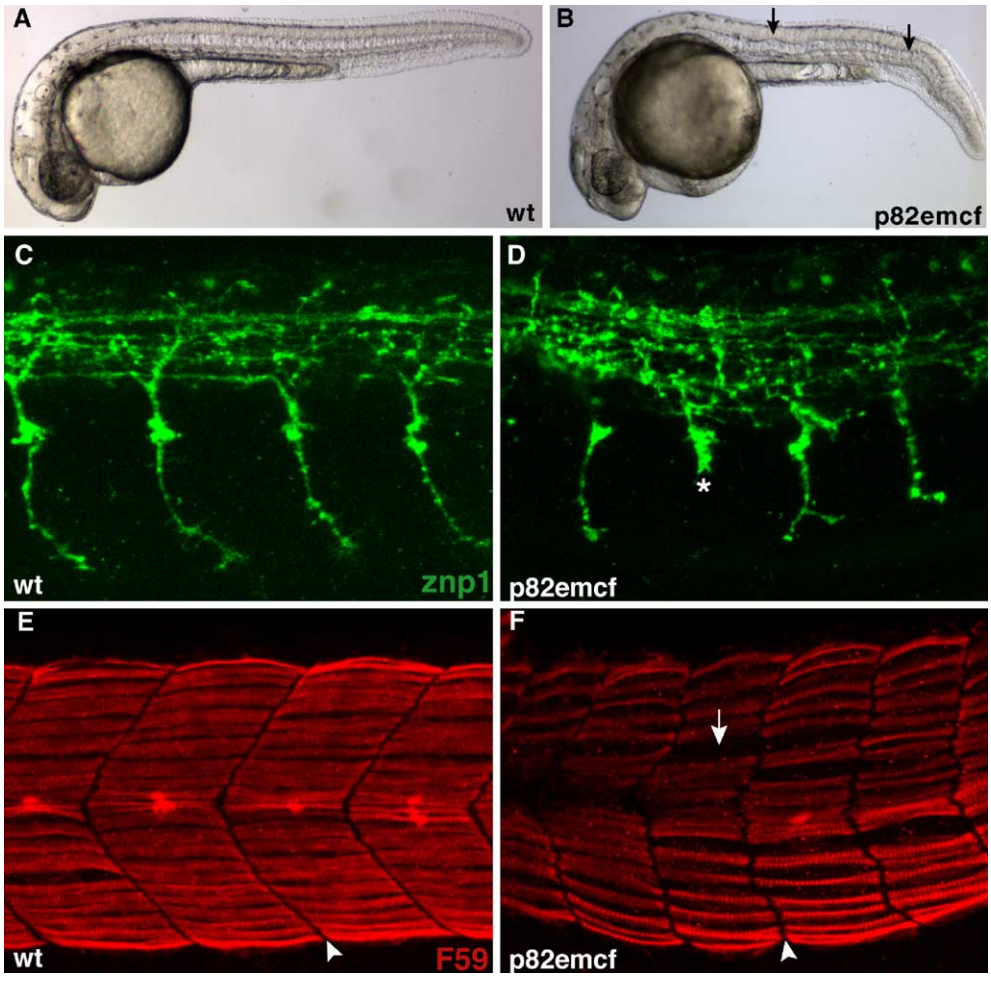

Fig. 7. Lateral on a wild-type and a p82emcf mutant embryo. Note the local bulging in the notochord (arrows). Lateral confocal images of wild-type (C, E) and mutant embryos (D, F) double stained with F59 for adaxial cells/slow muscle fibers and znp1 for motor axons. In panel D, an asterisk indicates a stumpy axon, and in panel F, an arrowhead points to irregular somites boundaries, and an arrow to gaps in the muscle fibers.

or branch at the choice point, while adaxial cells/slow muscle fibers are unaffected (Figs. 8A, B, and data not shown). This phenotype is reminiscent of what has been reported for *unplugged* mutants (Zhang and Granato, 2000). Complementation analysis and sequencing of the *unplugged* coding region from *p31cd* mutant embryos revealed that *p31cd* is a novel allele of *unplugged*. The *unplugged* gene encodes a MuSK like receptor tyrosine kinase, whose function in dorsal adaxial cells is essential for two of the three primary motor growth cones to make a pathfinding decision at a somitic choice point (Zhang and Granato, 2000; Zhang et al., 2004).

Identification of a novel *unplugged* allele provides two important insights. First, the new *unplugged* allele validates our screen, demonstrating that the sensitivity is sufficiently high to detect subtle axonal phenotypes, such as the ones present in *unplugged* mutants. Second, the *unplugged*^{p31cd} allele suggests unexpected ligands to activate *unplugged* signaling. Specifically, the *unplugged*^{p31cd} allele harbors a missense mutation in the *frizzled* like cysteine rich domain (CRD). This domain is critical for frizzled receptors to bind their Wnt ligands and has also been identified in a number of non-frizzled proteins, including MuSK family members (Bhanot et al., 1996; Xu and Nusse, 1998). In the *unplugged*^{p31cd} allele, the fourth of the 10 cysteines that defines the CR domain is altered to a tyrosine (C371Y). In *frizzled* receptors, tripeptide insertions just preceeding this fourth cysteine abolish ligand binding, underscoring the importance of the fourth cysteine in ligand binding (Dann et al., 2001; Hsieh et al., 1999). We have recently shown that *unplugged* function for pathfinding is independent of Agrin, a key activator of mammalian MuSK (Zhang et al., 2004). Thus, identification of the *unplugged*^{p31cd} allele supports the intriguing possibility that a Wnt signal may activate the *unplugged* receptor tyrosine kinase, thereby enabling motor axons to choose their path.

We identified two mutants, *p55emcf* and *p24cree*, that display phenotypes similar to each other. As these two mutants fail to complement each other, they affect the same gene, which we named *sidetracked* (*set*). In *set* mutants, adaxial cells/slow muscle fibers are unaffected, while motor axons in 40 to 60% of somitic hemisegments display one or

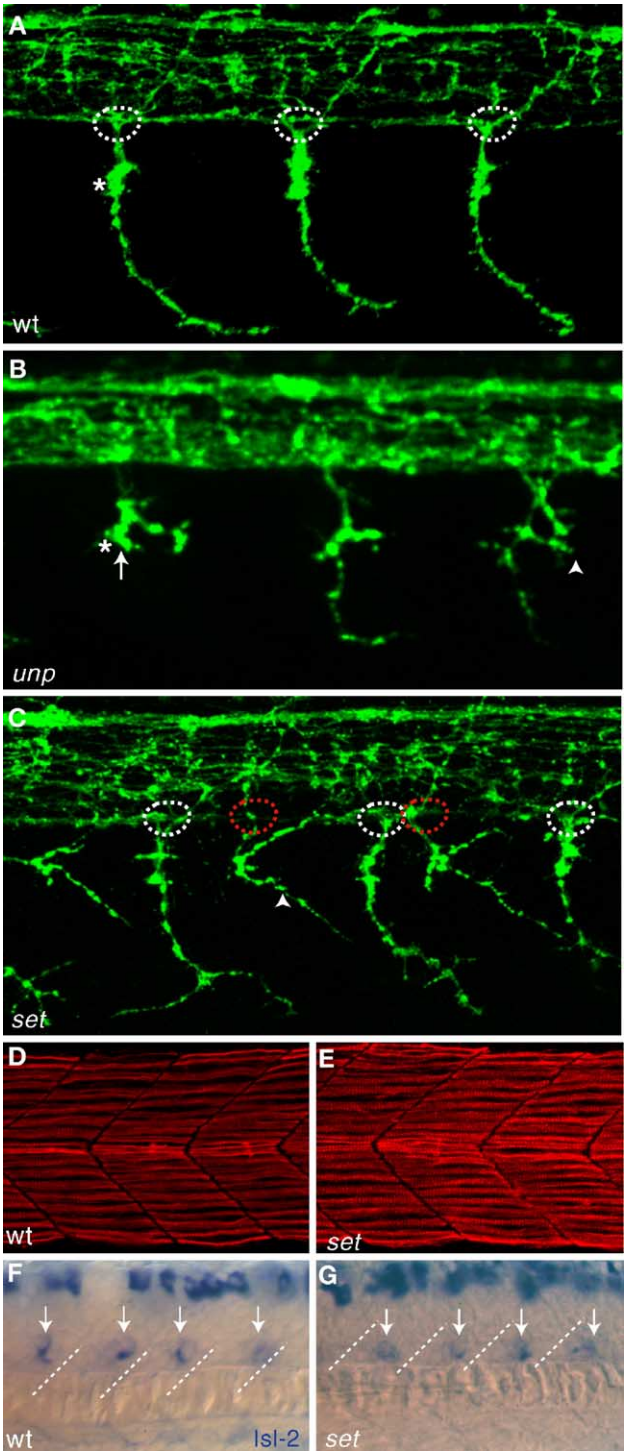

Fig. 8. Lateral confocal images of wild-type (A, D, F) and mutant embryos (B, C, E, G) stained with znp1 for motor axons (A–C) and with F59 for adaxial cells/slow muscle fibers (D, E), or for Isl2 (F, G). White dashed circles outline the segmental exit points, and asterisks the choice point. In panel B, an arrow points to a stalled axon, and an arrowhead to a branched axon. In panel C, note the ectopic exit points, marked by red circles. In panels F and G, somite boundaries are outlined by dashed lines, and arrows point to individual CaP motoneurons.

two pathfinding defects (Fig. 8C). First, in about 30–45% of somitic hemisegments, motor axons branch just before or after the choice point. Second, in about 5 to 23% of the hemisegments, motor axons enter the somite through a second, ectopic ventral root in addition to entering through the midsegmental ventral root. In mutant embryos, somite boundary formation, a visible readout for somite polarity, and myotome patterning, as judged by F59 immunostainings, are indistinguishable from wild-type embryos (Figs. 8D, E). Furthermore, *set* primary motoneurons appeared properly specified and present in appropriate numbers and in their correct anterior–posterior location (Figs. 8F, G). Finally, *sidetracked* mutants do not display any other detectable morphological or behavioral defects. Together, the mutant phenotype suggests that the *set* gene plays a critical role early during the process of motor axonal pathfinding when pioneering motor growth cones navigate towards and through the segmental exit point.

One of the earliest events during motor axonal pathfinding occurs when motoneurons located at a given spinal level extend axonal growth cones towards and through a common segmental exit point. The molecular mechanisms underlying the complex and multistage process by which motor growth cones navigate towards the exit point, recognize it, then turn ventrally and eventually exit the spinal cord, are poorly understood. It is thought that segmental exit sites must be specified for axonal targeting, but the respective contributions of specialized cells outside the spinal cord and of neuroepithelial cells within the spinal cord are unclear (Niederlander and Lumsden, 1996; Vermeren et al., 2003). The axonal phenotype observed in *set* mutants is intriguing, because somite morphology and myotome differentiation appear unaffected. This is in contrast to *pac* (*cdh2*) mutants, in which some motor axons exit the spinal cord at ectopic points. This phenotype is associated with and most likely secondary to defects in slow muscle fiber development. In contrast, *set* mutants do not display any noticeable defects in slow muscle fiber development or organization and therefore provide a unique opportunity to define the molecular and cellular processes that guide motor axons towards and through segmental exit points.

Conclusion

The goal of this screen was to identify additional genes essential for motor axon pathfinding. Motor axon guidance is dependent on factors intrinsic to the neuron and growth cone but also requires extrinsic signals. A previous large-scale motility screen and a smaller scale antibody screen have identified only a handful of mutants with defects in axonal pathfinding (Beattie et al., 1999; Granato et al., 1996). Through the phenotypic analyses of two of these genes, *unplugged* and *diwanka*, it has become clear that a specific subpopulation of myotomal cells, the adaxial cells, located along the future axonal path plays a major role in

providing essential extrinsic guidance cues (Zeller and Granato, 1999; Zeller et al., 2002; Zhang and Granato, 2000).

Combined, the results from our screen suggest three points. First, the distribution of mutants supports the notion that adaxial cells play a critical role in motor axonal pathfinding: six of the nine mutants with motor axonal defects also displayed defects in adaxial cell development. Each of the six mutants represents a mutant class previously isolated based on morphological defects. Re-identification of these previously known mutants might be seen as a major disadvantage but can provide novel insights into the biology of the affected gene. For example, *p32cqeg* mutants, which are member of the 'dwarf' group mutants, reveal a previously unrecognized role for 'dwarf' group genes in activity dependent motor axonal pathfinding and slow muscle fiber development. It is also interesting to note that some of the mutants with axonal and adaxial defects are caused by mutations in components of major signaling pathway in the embryos (*pac des*). For example, *des* (*notch1*α) plays a critical role in somite formation (Holley et al., 2002), and *des* (*notch1*α) mutants display, in addition to defects in somite development, defects in motor axonal pathfinding (Beattie et al., 1999; Granato et al., 1996). This might suggest that the effects of genes such as *des* (*notch1*α) on axonal guidance are indirect, i.e. secondary to somite patterning. However, in *Drosophila*, Notch is present on growth cones of extending motor axons and is critical for a specific guidance decision (Crowner et al., 2003; Giniger, 1998). Thus, zebrafish mutants in components of major signaling pathways need to be reexamined to determined if these signaling pathways play a direct role in vertebrate motor axon guidance (Beattie et al., 1999; Gray et al., 2001).

Second, antibody-based screens can identify mutations in presumptive guidance genes, without associated defects in morphology or locomotion. We find that 20% (3 out of 15) of the mutants do not have any additional phenotypes and would be undetectable in morphological screens. These mutants represent a small fraction, perhaps because one selects for genes that play a single, critical role during development. Finally, analyses of those mutants without additional phenotypes suggest that they define key entry points into biological processes not well understood, such as differentiation of muscle cell types towards their unique fiber type profile (*pop* mutants) or axonal guidance towards and through segmental central nervous system exit points (*set* mutants).

Acknowledgments

We would like to thank Michael Gyda for labeling RGCs, Shuxia Zhao for sequence analysis of the *unplugged* ^{p31cd} allele, Marnie Halpern and Rachel Brewster for N-cadherin primers and Julie Lefebvre for *unplugged* ^{p31cd} znp1 stainings. We would also like to thank Mary Halloran (University of Wisconsin, Madison) for performing complementation with *bashful*, and Rolf Karlstrom (University of Massachusetts, Amherst) for providing *chameleon* fish. This work was supported by grants from the Muscle Dystrophy Association of America (M.G.) and the National Institute of Health to (M.C.M, M.G.).

References

Amsterdam, A., Nissen, R.M., Sun, Z., Swindell, E.C., Farrington, S., Hopkins, N., 2004. Identification of 315 genes essential for early zebrafish development. Proc. Natl. Acad. Sci. U. S. A 101, 12792–12797.

Barresi, M.J., Stickney, H.L., Devoto, S.H., 2000. The zebrafish slow-muscle-omitted gene product is required for Hedgehog signal transduction and the development of slow muscle identity. Development 127, 2189–2199.

Barresi, M.J., D'Angelo, J.A., Hernandez, L.P., Devoto, S.H., 2001. Distinct mechanisms regulate slow-muscle development. Curr. Biol. 11, 1432–1438.

Baxendale, S., Davison, C., Muxworthy, C., Wolff, C., Ingham, P.W., Roy, S., 2004. The B-cell maturation factor Blimp-1 specifies vertebrate slow-twitch muscle fiber identity in response to Hedgehog signaling. Nat. Genet. 36, 88–93.

Beattie, C.E., 2000. Control of motor axon guidance in the zebrafish embryo. Brain Res. Bull. 53, 489–500.

Beattie, C.E., Raible, D.W., Henion, P.D., Eisen, J.S., 1999. Early pressure screens. Methods Cell Biol. 60, 71–86.

Beattie, C.E., Melancon, E., Eisen, J.S., 2000. Mutations in the stumpy gene reveal intermediate targets for zebrafish motor axons. Development 127, 2653–2662.

Bernhardt, R.R., Goerlinger, S., Roos, M., Schachner, M., 1998. Anterior–posterior subdivision of the somite in embryonic zebrafish: implications for motor axon guidance. Dev. Dyn. 213, 334–347.

Bhanot, P., Brink, M., Samos, C.H., Hsieh, J.C., Wang, Y., Macke, J.P., Andrew, D., Nathans, J., Nusse, R., 1996. A new member of the frizzled family from *Drosophila* functions as a Wingless receptor. Nature 382, 225–230.

Chappuis-Flament, S., Wong, E., Hicks, L.D., Kay, C.M., Gumbiner, B.M., 2001. Multiple cadherin extracellular repeats mediate homophilic binding and adhesion. J. Cell Biol. 154, 231–243.

Cohen, M.W., Greschner, M., Tucci, M., 1984. In vivo development of cholinesterase at a neuromuscular junction in the absence of motor activity in *Xenopus laevis*. J. Physiol. 348, 57–66.

Cortes, F., Daggett, D., Bryson-Richardson, R.J., Neyt, C., Maule, J., Gautier, P., Hollway, G.E., Keenan, D., Currie, P.D., 2003. Cadherin-mediated differential cell adhesion controls slow muscle cell migration in the developing zebrafish myotome. Dev. Cell 5, 865–876.

Crow, M.T., Stockdale, F.E., 1986. Myosin expression and specialization among the earliest muscle fibers of the developing avian limb. Dev. Biol. 113, 238–254.

Crowner, D., Le Gall, M., Gates, M.A., Giniger, E., 2003. Notch steers *Drosophila* ISNb motor axons by regulating the Abl signaling pathway. Curr. Biol. 13, 967–972.

Currie, P.D., Ingham, P.W., 1996. Induction of a specific muscle cell type by a hedgehog-like protein in zebrafish. Nature 382, 452–455.

Dann, C.E., Hsieh, J.C., Rattner, A., Sharma, D., Nathans, J., Leahy, D.J., 2001. Insights into Wnt binding and signalling from the structures of two Frizzled cysteine-rich domains. Nature 412, 86–90.

Devoto, S.H., Melancon, E., Eisen, J.S., Westerfield, M., 1996. Identification of separate slow and fast muscle precursor cells in vivo, prior to somite formation. Development 122, 3371–3380.

Dosch, R., Wagner, D.S., Mintzer, K.A., Runke, G., Wiemelt, A.P., Mullins, M.C., 2004. Maternal control of vertebrate development before the midblastula transition: mutants from the zebrafish I. Dev. Cell 6, 771–780.

Driever, W., Solnica-Krezel, L., Schier, A.F., Neuhauss, S.C.F., Malicki, J.,

Stemple, D.L., Stainier, D.Y.R., Zwartkruis, F., Abdelilah, S., Rangini, Z., Belak, J., Boggs, C., 1996. A genetic screen for mutations affecting embryogenesis in zebrafish. Development 123, 37–346.

Eisen, J.S., Myers, P.Z., Westerfield, M., 1986. Pathway selection by growth-cones of identified motoneurons in live zebra fish embryos. Nature 320, 269–271.

Felsenfeld, A.L., Curry, M., Kimmel, C.B., 1991. The fub-1 mutation blocks initial myofibril formation in zebrafish muscle pioneer cells. Dev. Biol. 148, 23–30.

Forrester, W.C., Garriga, G., 1997. Genes necessary for *C. elegans* cell and growth cone migrations. Development 124, 1831–1843.

Fricke, C., Lee, J.S., Geiger-Rudolph, S., Bonhoeffer, F., Chien, C.B., 2001. Astray, a zebrafish roundabout homolog required for retinal axon guidance. Science 292, 507–510.

Giniger, E., 1998. A role for Abl in Notch signaling. Neuron 20, 667–681.

Glasgow, E., Tomarev, S.I., 1998. Restricted expression of the homeobox gene prox-1 in developing zebrafish. Mech. Dev., 175–178.

Granato, M., van Eeden, F.J.M., Schach, U., Trowe, T., Brand, M., Furutani-Seiki, M., Haffter, P., Hammerschmidt, M., Heisenberg, C.-P., Jiang, Y.-J., Kane, D.A., Kelsh, R.N., Mullins, M.C., Odenthal, J., Nüsslein-Volhard, C., 1996. Genes controlling and mediating locomotion behaviour of the zebrafish embryo and larva. Development 123, 399–413.

Gray, M., Moens, C.B., Amacher, S.L., Eisen, J.S., Beattie, C.E., 2001. Zebrafish deadly seven functions in neurogenesis. Dev. Biol. 237, 306–323.

Haffter, P., Granato, M., Brand, M., Mullins, M.C., Hammerschmidt, M., Kane, D.A., Odenthal, J., van Eeden, F.J.M., Jiang, Y.-J., Heisenberg, C.-P., Kelsh, R.N., Furutani-Seiki, M., Vogelsang, E., Beuchle, D., Schach, U., Fabian, C., Nüsslein-Volhard, C., 1996. The identification of genes with unique and essential functions in the development of the zebrafish, *Danio rerio*. Development 123, 1–36.

Halpern, M.E., Ho, R.K., Walker, C., Kimmel, C.B., 1993. Induction of muscle pioneers and floor plate is distinguished by the zebrafish no tail mutation. Cell 75, 99–111.

Hatta, K., Bremiller, R., Westerfield, M., Kimmel, C.B., 1991. Diversity of expression of engrailed-like antigens in zebrafish. Development 112, 821–832.

Holley, S.A., Julich, D., Rauch, G.J., Geisler, R., Nusslein-Volhard, C., 2002. her1 and the notch pathway function within the oscillator mechanism that regulates zebrafish somitogenesis. Development 129, 1175–1183.

Hsieh, J.C., Rattner, A., Smallwood, P.M., Nathans, J., 1999. Biochemical characterization of Wnt-frizzled interactions using a soluble, biologically active vertebrate Wnt protein. Proc. Natl. Acad. Sci. U. S. A. 96, 3546–3551.

Jiang, Y.-J., Brand, M., Heisenberg, C.-P., Beuchle, D., Furutani-Seiki, M., Kelsh, R.N., Warga, R.M., Granato, M., Haffter, P., Hammerschmidt, M., Kane, D.A., Mullins, M.C., Odenthal, J., van Eeden, F.J.M., Nüsslein-Volhard, C., 1996. Mutations affecting neurogenesis and brain morphology in the zebrafish, *Danio rerio*. Development 123, 205–216.

Karlstrom, R.O., Trowe, T., Klostermann, S., Baier, H., Brand, M., Crawford, A.D., Grunewald, B., Haffter, P., Hoffman, H., Meyer, S.U., Müller, B.K., Richter, S., van Eeden, F.J.M., Nüsslein-Volhard, C., Bonhoeffer, F., 1996. Zebrafish mutations affecting retinotectal axon pathfinding. Development 123, 427–438.

Karlstrom, R.O., Talbot, W.S., Schier, A.F., 1999. Comparative synteny cloning of zebrafish you-too: mutations in the Hedgehog target gli2 affect ventral forebrain patterning. Genes Dev. 13, 388–393.

Kimmel, C.B., Ballard, W.W., Kimmel, S.R., Ullmann, B., Schilling, T., 1995. Stages of embryonic development of the zebrafish. Dev. Dyn. 203, 253–310.

Kraut, R., Menon, K., Zinn, K., 2001. A gain-of-function screen for genes controlling motor axon guidance and synaptogenesis in *Drosophila*. Curr. Biol. 11, 417–430.

Lefebvre, J.L., Ono, F., Puglielli, C., Seidner, G., Franzini-Armstrong, C., Brehm, P., Granato, M., 2004. Increased neuromuscular activity causes axonal defects and muscular degeneration. Development 131, 2605–2618.

Leighton, P.A., Mitchell, K.J., Goodrich, L.V., Lu, X., Pinson, K., Scherz, P., Skarnes, W.C., Tessier-Lavigne, M., 2001. Defining brain wiring patterns and mechanisms through gene trapping in mice. Nature 410, 174–179.

Lele, Z., Folchert, A., Concha, M., Rauch, G.J., Geisler, R., Rosa, F., Wilson, S.W., Hammerschmidt, M., Bally-Cuif, L., 2002. Parachute/n-cadherin is required for morphogenesis and maintained integrity of the zebrafish neural tube. Development 129, 3281–3294.

Lin, J., Wu, H., Tarr, P.T., Zhang, C.Y., Wu, Z., Boss, O., Michael, L.F., Puigserver, P., Isotani, E., Olson, E.N., Lowell, B.B., Bassel-Duby, R., Spiegelman, B.M., 2002. Transcriptional co-activator PGC-1 alpha drives the formation of slow-twitch muscle fibres. Nature 418, 797–801.

Malicki, J., Jo, H., Pujic, Z., 2003. Zebrafish N-cadherin, encoded by the glass onion locus, plays an essential role in retinal patterning. Dev. Biol. 259, 95–108.

Masai, I., Lele, Z., Yamaguchi, M., Komori, A., Nakata, A., Nishiwaki, Y., Wada, H., Tanaka, H., Nojima, Y., Hammerschmidt, M., Wilson, S.W., Okamoto, H., 2003. N-cadherin mediates retinal lamination, maintenance of forebrain compartments and patterning of retinal neurites. Development 130, 2479–2494.

Melançon, E., Liu, D.W.C., Westerfield, M., Eisen, J.S., 1997. Pathfinding by identified zebrafish motorneurons in the absence of muscle poineers. J. Neurosci. 17, 7796–7804.

Morck, C., Axang, C., Pilon, M., 2003. A genetic analysis of axon guidance in the *C. elegans* pharynx. Dev. Biol. 260, 158–175.

Mullins, M.C., Hammerschmidt, M., Haffter, P., Nüsslein-Volhard, C., 1994. Large-scale mutagenesis in the zebrafish: in search of genes controlling development in a vertebrate. Curr. Biol. 4, 189–202.

Myers, P.Z., Eisen, J.S., Westerfield, M., 1986. Development and axonal outgrowth of identified motoneurons in the zebrafish. J. Neurosci. 6, 2278–2289.

Nakano, Y., Kim, H.R., Kawakami, A., Roy, S., Schier, A.F., Ingham, P.W., 2004. Inactivation of dispatched 1 by the chameleon mutation disrupts Hedgehog signalling in the zebrafish embryo. Dev. Biol. 269, 381–392.

Niederlander, C., Lumsden, A., 1996. Late emigrating neural crest cells migrate specifically to the exit points of cranial branchiomotor nerves. Development 122, 2367–2374.

Odenthal, J., Haffter, P., Vogelsang, E., Brand, M., van Eeden, F.J.M., Furutani-Seiki, M., Granato, M., Hammerschmidt, M., Heisenberg, C.-P., Jiang, Y.-J., Kane, D.A., Kelsh, R.N., Mullins, M.C., Warga, R.M., Allende, M.L., Weinberg, E.S., Nüsslein-Volhard, C., 1996. Mutations affecting the formation of the notochord in the zebrafish, *Danio rerio*. Development 123, 103–115.

Parsons, M.J., Pollard, S.M., Saude, L., Feldman, B., Coutinho, P., Hirst, E.M., Stemple, D.L., 2002. Zebrafish mutants identify an essential role for laminins in notochord formation. Development 129, 3137–3146.

Patton, B.L., 2000. Laminins of the neuromuscular system. Microsc. Res. Tech. 51, 247–261.

Patton, B.L., Cunningham, J.M., Thyboll, J., Kortesmaa, J., Westerblad, H., Edstrom, L., Tryggvason, K., Sanes, J.R., 2001. Properly formed but improperly localized synaptic specializations in the absence of laminin alpha4. Nat. Neurosci. 4, 597–604.

Rodino-Klapac, L.R., Beattie, C.E., 2004. Zebrafish topped is required for ventral motor axon guidance. Dev. Biol. 273, 308–320.

Schauerte, H.E., van Eeden, F.J.M., Fricke, C., Odenthal, J., Strahle, U., Haffter, P., 1998. Sonic hedgehog is not required for the induction of medial floor plate cells in the zebrafish. Development 125, 2983–2993.

Seeger, M., Tear, G., Ferres-Marco, D., Goodman, C.S., 1993. Mutations affecting growth cone guidance in *Drosophila*: genes necessary for guidance toward or away from the midline. Neuron 10, 409–426.

Stemple, D.L., Solnica-Krezel, L., Zwartkruis, F., Neuhauss, S.C.F., Schier, A.F., Malicki, J., Stainier, D.Y.R., Abdelilah, S., Rangini, Z.,

Mountcastle-Shah, E., Driever, W., in press. Mutations affecting development of the notochord in zebrafish. Development.

Stickney, H.L., Barresi, M.J., Devoto, S.H., 2000. Somite development in zebrafish. Dev. Dyn. 219, 287–303.

Trevarrow, B., Marks, D.L., Kimmel, C.B., 1990. Organization of hindbrain segments in the zebrafish embryo. Neuron 4, 669–679.

van Eeden, F.J.M., Granato, M., Schach, U., Brand, M., Furutani-Seiki, M., Haffter, P., Hammerschmidt, M., Heisenberg, C.-P., Jiang, Y.-J., Kane, D.A., Kelsh, R.N., Mullins, M.C., Odenthal, J., Warga, R.M., Allende, M.L., Weinberg, E.S., Nüsslein-Volhard, C., 1996. Mutations affecting somite formation and patterning in the zebrafish *Danio rerio*. Development 123, 153–164.

Van Vactor, D., Sink, H., Fambrough, D., Tsoo, R., Goodman, C., 1993. Genes that control neuromuscular specificity in *Drosophila*. Cell 73, 1137–1153.

Vermeren, M., Maro, G.S., Bron, R., McGonnell, I.M., Charnay, P., Topilko, P., Cohen, J., 2003. Integrity of developing spinal motor columns is regulated by neural crest derivatives at motor exit points. Neuron 37, 403–415.

Westerfield, M., McMurray, J.V., Eisen, J.S., 1986. Identified motoneurons and their innervation of axial muscles in the zebrafish. J. Neurosci. 6, 2267–2277.

Wightman, B., Baran, R., Garriga, G., 1997. Genes that guide growth cones along the *C. elegans* ventral nerve cord. Development 124, 2571–2580.

Wolff, C., Roy, S., Ingham, P.W., 2003. Multiple muscle cell identities induced by distinct levels and timing of hedgehog activity in the zebrafish embryo. Curr. Biol. 13, 1169–1181.

Xu, Y.K., Nusse, R., 1998. The Frizzled CRD domain is conserved in diverse proteins including several receptor tyrosine kinases. Curr. Biol. 8, R405–R406.

Zallen, J.A., Kirch, S.A., Bargmann, C.I., 1999. Genes required for axon pathfinding and extension in the *C. elegans* nerve ring. Development 126, 3679–3692.

Zeller, J., Granato, M., 1999. The zebrafish diwanka gene controls an early step of motor growth cone migration. Development 126, 3461–3472.

Zeller, J., Schneider, V., Malayaman, S., Higashijima, S., Okamoto, H., Gui, J., Lin, S., Granato, M., 2002. Migration of zebrafish spinal motor nerves into the periphery requires multiple myotome-derived cues. Dev. Biol. 252, 241–256.

Zhang, J., Granato, M., 2000. The zebrafish unplugged gene controls motor axon pathway selection. Development 127, 2099–2111.

Zhang, J., Malayaman, S., Davis, C., Granato, M., 2001. A dual role for the zebrafish unplugged gene in motor axon pathfinding and pharyngeal development. Dev. Biol. 240, 560–573.

Zhang, J., Lefebvre, J.L., Zhao, S., Granato, M., 2004. Zebrafish unplugged reveals a role for muscle-specific kinase homologs in axon pathway choice. Nature Neuroscience 7, 1303–1309.